Journal of Energy Technologies and Policy
ISSN 2224-3232 (Paper) ISSN 2225-0573 (Online)
Vol.5, No.4, 2015

Effects of Pressure and Heating Rate on Products Release Rates and Yields during Biomass Pyrolysis in Thermally Thick Regime

Pious O. Okekunle* and Daniel I. Adeniranye

Department of Mechanical Engineering, Faculty of Engineering and Technology,
Ladoke Akintola University of Technology, P.M.B. 4000, Ogbomoso, Oyo state, Nigeria.

*Email of the corresponding author: pookekunle@lautech.edu.ng

Abstract

Numerical investigation of the synergetic effects of reactor pressure and heating rate on biomass pyrolysis in thermally thick regime has been carried out. Wood cylinders ($\rho = 400\ kg/m^3$, $\emptyset\ 10\ mm$ and length $20\ mm$) were modeled as two-dimensional porous solids. Transport equations, solid mass conservation equations, intra-particle pressure generation equation and energy conservation equation were coupled and simultaneously solved to simulate the pyrolysis process and the accompanying physical phenomena. First order Euler Implicit Method (EIM) was used to solve the solid mass conservation equations. The transport, energy conservation and intra-particle pressure generation equations were discretized by Finite Volume Method (FVM). The generated set of linear equations was solved by Tri-Diagonal Matrix Algorithm (TDMA). Intra-particle fluid flow velocity was estimated by Darcy's law. Findings revealed that increase in reactor pressure does not significantly affect biomass primary decomposition reactions for all heating rates considered (10, 20, 30, 40 and 50 K/s). In the vacuum region (0.0001 and 0.01 atm), increase in pressure had no significant effect on the release rates and yields of product species at all heating rates. In the pressurized region, increase in pressure (from 10 to 100 atm) inhibited intra-particle secondary reactions. Pressure increase from vacuum to atmospheric and from atmospheric to pressurized condition caused some changes in product distribution. The degrees of intra-particle secondary reactions at atmospheric and pressurized conditions were much higher than at vacuum conditions. Primary tar release rates and yields at atmospheric and pressurized conditions were much lower than at vacuum conditions while gas and secondary tar release rates and yields were higher at atmospheric and pressurized conditions. Intra-particle secondary reactions were more sensitive to change in heating rate at vacuum conditions than at atmospheric and pressurized conditions.

Keywords: Biomass, pyrolysis, pressure, heating rate, intra-particle secondary reactions, thermally thick regime

1. Introduction

Biomass has been recognized as a potential source of energy for sustainable development. Unlike conventional fossil fuels, biomass is carbon neutral and therefore portends no threat to the environment. Many research works have been done on biomass pyrolysis in order to better understand various accompanying phenomena [1-13]. The reaction kinetics, heat, mass and momentum transfers during pyrolysis are all affected by the operating conditions, feedstock type [14] and configurations [15], and reactor type [16]. More often than not, the yield of a product is given preference over others in a particular experiment. This therefore calls for some in-depth knowledge on how various process parameters affect products release rates and yields. Of recent, the combined impact of reactor pressure and heating rate on evolution and yields of biomass pyrolysis products in thermally thin regime was investigated [17]. Synergetic effect of these parameters on intra-particle secondary reactions was also analyzed. Findings revealed that total tar yield decreased as pressure increased from vacuum to atmospheric and from atmospheric to pressurized condition at all heating rates considered. The need to consider thermally thick pyrolysis regime is borne out of the fact that most commercial biomass thermochemical conversion plants make use of samples in this regime [18]. In this regime, intra-particle temperature distribution is no longer uniform. Although some researchers have modeled and simulated the nature of pyrolysis product yield distribution and composition in this regime [13,19], a handful has considered the combined effect of pressure and heating rate on pyrolysis characteristics. This research work was intended to fill this gap.

Synergetic effects of pressure and heating rate on weight loss history, primary and secondary reactions rates, volatiles release rates and yields, and temperature evolution at the centre of the pyrolyzing solid were simulated. Results were also furnished with the total yield of product species.

2. Pyrolysis Mechanism

Figure 1 shows the structure of the pyrolysis mechanism adopted in this study. A detailed explanation on the development of this mechanism has been reported in our earlier research works [20, 21]. As shown in the figure, wood first decomposes by three endothermic competing primary reactions to form gas, primary tar and intermediate solid. The primary tar undergoes secondary reactions to yield more gas and char. The intermediate solid is further transformed into char by a strong exothermic reaction as shown in the figure. Reaction rates were assumed to follow Arrhenius expression of the form; $k_i = A_i \exp\left(-E_i/RT\right)$. The chemical kinetic ($A$ and E) and thermodynamic (a and b) parameters are as given in one of our previous works [21].

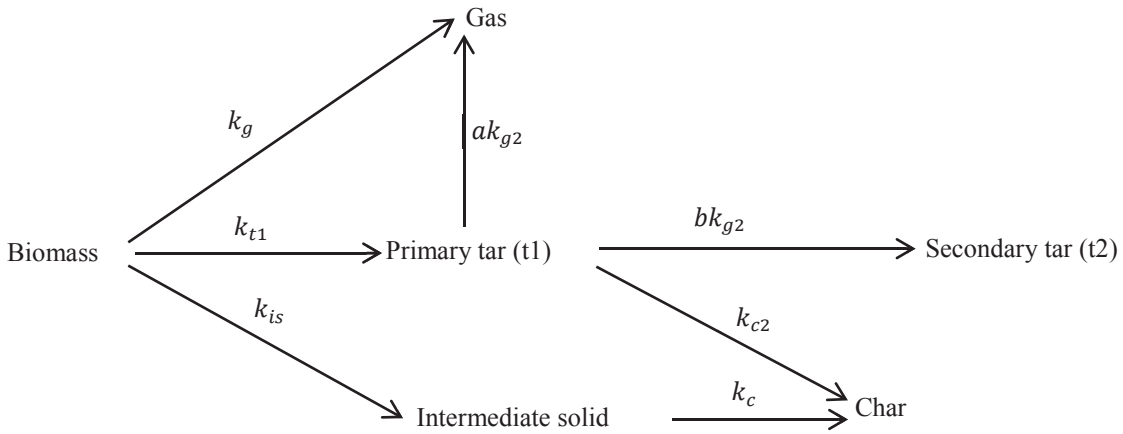

Figure 1: Schematic illustration of pyrolysis mechanism

3. Numerical simulation

The governing equations, model assumptions and numerical procedures in this study are already given in our previous studies [20, 21, 12]. Therefore, fundamental governing equations are only given here.

3.1 Solid mass conservation equations

The instantaneous mass balance of the pyrolyzing solid comprises three endothermic consumption terms yielding gas, primary tar and intermediate solid, given as

$$\frac{\partial \rho_s}{\partial t} = -(k_g + k_t + k_{is})\rho_s \quad (1)$$

The intermediate solid instantaneous mass balance equation (equation (2)) contains two terms, one for the conversion of the virgin solid to intermediate solid and the other from exothermic decomposition of intermediate solid to yield char, given as

$$\frac{\partial \rho_{is}}{\partial t} = k_{is}\rho_s - k_c\rho_{is} \quad (2)$$

Also, the char instantaneous mass balance equation (equation(3)) contains two terms, one from the exothermic decomposition of intermediate solid and the other from primary tar secondary reaction to yield char, given as

$$\frac{\partial \rho_c}{\partial t} = k_c\rho_{is} + k_{c2}\rho_t \quad (3)$$

3.2 Mass conservation equations of gas phase components

Mass conservation equations for all gas phase components are expressed by two-dimensional cylindrical coordinate system consisting of both temporal and spatial gradients and source terms, given by

$$\text{Ar: } \frac{\partial(\varepsilon\rho_{Ar})}{\partial t} + \frac{\partial(\rho_{Ar}U)}{\partial z} + \frac{1}{r}\frac{\partial(r\rho_{Ar}V)}{\partial r} = S_{Ar}, \tag{4}$$

$$\text{Gas: } \frac{\partial(\varepsilon\rho_{g})}{\partial t} + \frac{\partial(\rho_{g}U)}{\partial z} + \frac{1}{r}\frac{\partial(r\rho_{g}V)}{\partial r} = S_{g}, \tag{5}$$

$$\text{Primary tar : } \frac{\partial(\varepsilon\rho_{t1})}{\partial t} + \frac{\partial(\rho_{t1}U)}{\partial z} + \frac{1}{r}\frac{\partial(r\rho_{t1}V)}{\partial r} = S_{t1}, \tag{6}$$

$$\text{Secondary tar: } \frac{\partial(\varepsilon\rho_{t2})}{\partial t} + \frac{\partial(\rho_{t2}U)}{\partial z} + \frac{1}{r}\frac{\partial(r\rho_{t2}V)}{\partial r} = S_{t2} \tag{7}$$

S_{Ar} , S_g, S_{t1} and S_{t2} are the source terms for the carrier gas (argon), gas, primary tar and secondary tar respectively, and are given by

$$S_{Ar} = 0 \tag{8}$$

$$S_g = k_g\rho_s + \varepsilon k_{g2}\rho_{t1} \tag{9}$$

$$S_{t1} = k_t\rho_s - \varepsilon[k_{c2} + (a+b)k_{g2}]\rho_{t1} \tag{10}$$

$$S_{t2} = \varepsilon b k_{g2}\rho_{t1} \tag{11}$$

Intra-particle tar and gas transport velocity was estimated by Darcy's law, given by

$$U = -\frac{B}{\mu}\left(\frac{\partial P}{\partial z}\right) \tag{12}$$

$$V = -\frac{B}{\mu}\left(\frac{\partial P}{\partial r}\right) \tag{13}$$

where B and μ are respectively the charring biomass solid permeability and kinematic viscosity. Porosity,ε, is expressed as

$$\varepsilon = 1 - \frac{\rho_{s,sum}}{\rho_{w,0}}(1 - \varepsilon_{w,0}) \tag{14}$$

where $\varepsilon_{w,0}$, $\rho_{s,sum}$ and $\rho_{w,0}$ are the initial porosity of wood, the sum of solid mass density and initial wood density, respectively. The permeability, B, of the charring biomass is expressed as a linear interpolation between the solid phase components, given as

$$B = (1 - \eta)B_w + \eta B_c \tag{15}$$

where η is the degree of pyrolysis and is defined as

$$\eta = 1 - \frac{\rho_s + \rho_{is}}{\rho_{w,0}} \tag{16}$$

3.3 Energy conservation equation

The energy conservation equation is given as

$$\left(C_{p,w}\rho_s + C_{p,w}\rho_{is} + C_{p,c}\rho_c + \varepsilon C_{p,t}\rho_{t1} + \varepsilon C_{p,t}\rho_{t2} + \varepsilon C_{p,g}\rho_g\right)\frac{\partial T}{\partial t} = \frac{\partial}{\partial z}\left(k_{eff(z)}\frac{\partial T}{\partial z}\right) + \frac{1}{r}\frac{\partial}{\partial r}\left(rk_{eff(r)}\frac{\partial T}{\partial r}\right) - l_c\Delta h_c - \sum_{i=g,t1,is} m_i\Delta h_i - \varepsilon\sum_{i=g2,t2,c2} n_i\Delta h_i \quad (17)$$

where

$$l_c = A_c \exp(-E_c/RT)\,\rho_{is} \quad (18)$$

$$m_i = A_i \exp(-E_i/RT)\,\rho_s \quad i = g, t1, is \quad (19)$$

$$n_i = A_i \exp(-E_i/RT)\,\rho_{t1} \quad i = g2, t2, c2 \quad (20)$$

The thermo-physical properties of the wood sample are as given in our previous study [22].

3.4 Pressure evolution

The total pressure is the sum of the partial pressures of the inert gas (argon), gas and secondary tar from the pyrolysis process. It is given as

$$P = P_{Ar} + P_{t2} + P_g;\;\; P_i = \frac{\rho_i RT}{M_i} \qquad (i = Ar, t2, g) \quad (21)$$

where M_i and R are the molecular weight of each gaseous species and universal gas constant, respectively. Combining equations (4), (5), (7), (12), (13) and (21), intra-particle pressure equation was obtained as

$$\frac{\partial}{\partial t}\left(\varepsilon\frac{P}{T}\right) - \frac{\partial}{\partial r}\left[\frac{BP}{\mu T}\left(\frac{\partial P}{\partial z}\right)\right] - \frac{1}{r}\frac{\partial}{\partial r}\left[r\frac{BP}{\mu T}\left(\frac{\partial P}{\partial r}\right)\right] = \frac{R}{M_{t2}}S_{t2} + \frac{R}{M_g}S_g \quad (22)$$

3.5 Numerical Procedure

Wood pellets were modeled as two-dimensional porous solids. Wood pores were assumed to be initially filled with argon. As the solid was pyrolyzed, tar and gas were formed while argon was displaced to the outer region without participating in the pyrolysis reaction. The solid mass conservation equations (eqs (1) – (3)) were solved by first-order Euler Implicit Method. The mass conservation equations for argon, primary tar, gas and secondary tar (eqs (4) – (7)), energy conservation equation (eq. (17)) and the pressure equation (eq. (22)) were discretized using Finite Volume Method (FVM). Hybrid differencing scheme was adopted for the convective terms. First-order fully implicit scheme was used for the time integral with a time step of 0.005 s. The detailed numerical procedure and calculation domain have been given somewhere else [20]. Model assumptions have also been given previously [12].

4. Results and discussion

4.1 Pressure and heating rate effects on weight fraction history

Figure 2 [a-e] shows the weight loss history of the pyrolyzing solid at different heating rates (10, 20, 30, 40 and 50 K/s) and at vacuum (0.0001 and 0.01 atm), atmospheric (1 atm) and pressurized (10 and 100 atm) pyrolysis regions. As seen from the figure, increase in heating rate enhanced the rate of biomass decomposition in all pyrolysis pressure regions considered. It can also be clearly seen that increase in heating rate produced the same effects in all the pressure regions considered. This scenario has been observed in thermally thin regime [17]. However, commencement of significant biomass decomposition took a much longer time than in thermally thin regime. This was because longer time is required in this regime for particle heat up and moisture evaporation before the initiation of primary decomposition reactions. Furthermore, emergence of spatial (intra-particle) temperature gradient in this regime made the pyrolysis reaction front gradually advance into the interior of the solid thereby making the weight loss gradient lesser than in thermally thin regime. This was observed in all pressure regions considered as shown in the figure. Moreover, the figure also shows that the weight loss histories for all heating rates at different pyrolysis pressures were similar. This implies that reactor pressure has no

significant effect on biomass primary decomposition reactions except for some time elongation especially at 100 atm.

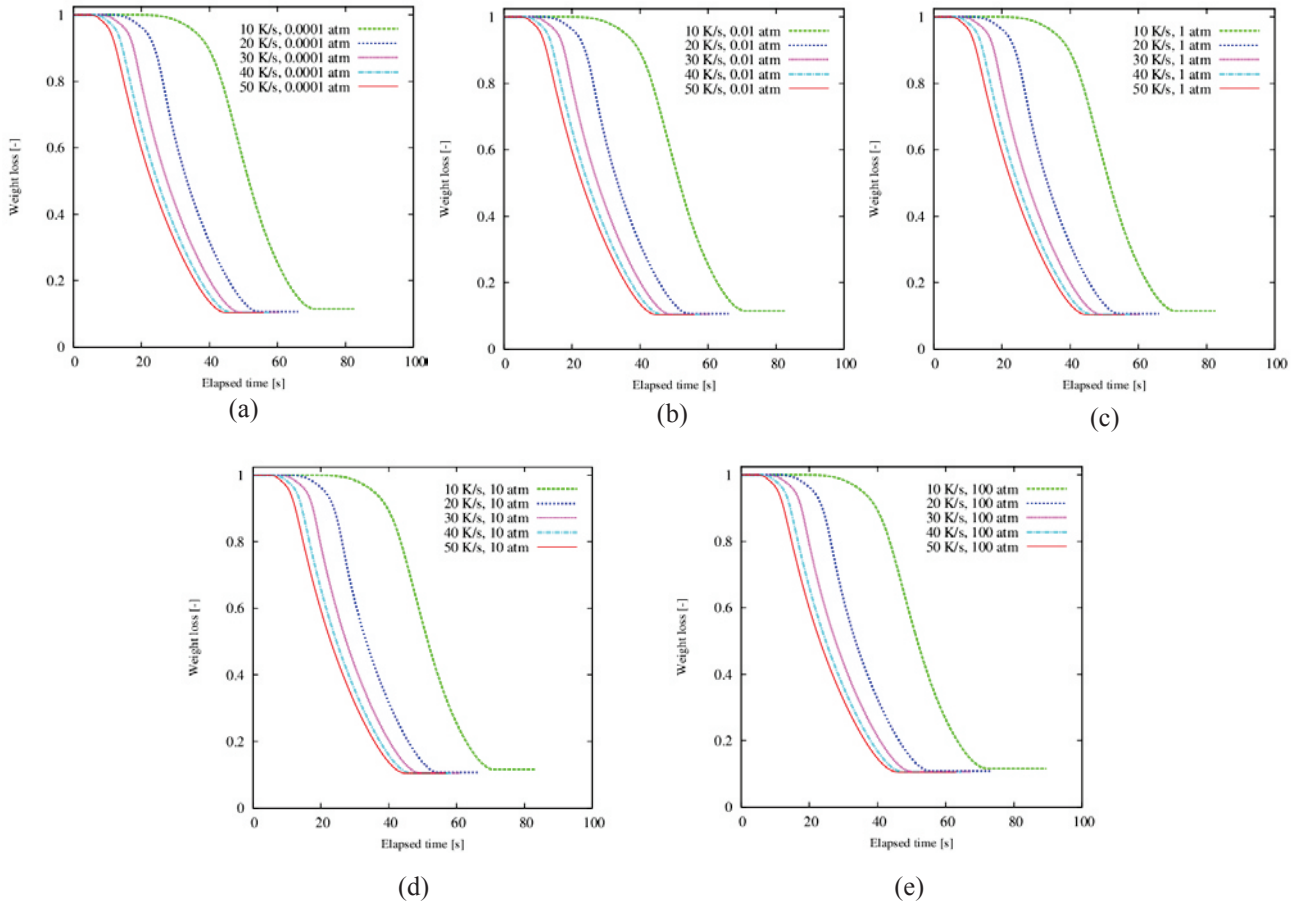

Figure 2: Weight loss history at different reactor pressures and heating rates

4.2 Primary tar generation rate

The complexity of tarry compounds and their potential to participate in both intra-particle and extra-particle vapour- phase secondary reactions have made their evolution mechanism, reaction kinetics, and intra- and extra-particle transport of great interest to researchers [23]. In this work, an attempt was also made to simulate the rate of evolution of primary tar from wood primary decomposition reaction. Figure 3 [a-e] shows the production rate of primary tar at different heating rates in vacuum, atmospheric and pressurized pyrolysis conditions. From the figure, it is clearly seen that primary tar production rate increased with increasing heating rate at all pyrolysis pressure regions considered. However, increase in pressure, either from vacuum to atmospheric or from atmospheric to pressurized region had no significant effect on primary tar production rate. This observation has been made in our previous studies in thermally thin regime [17].

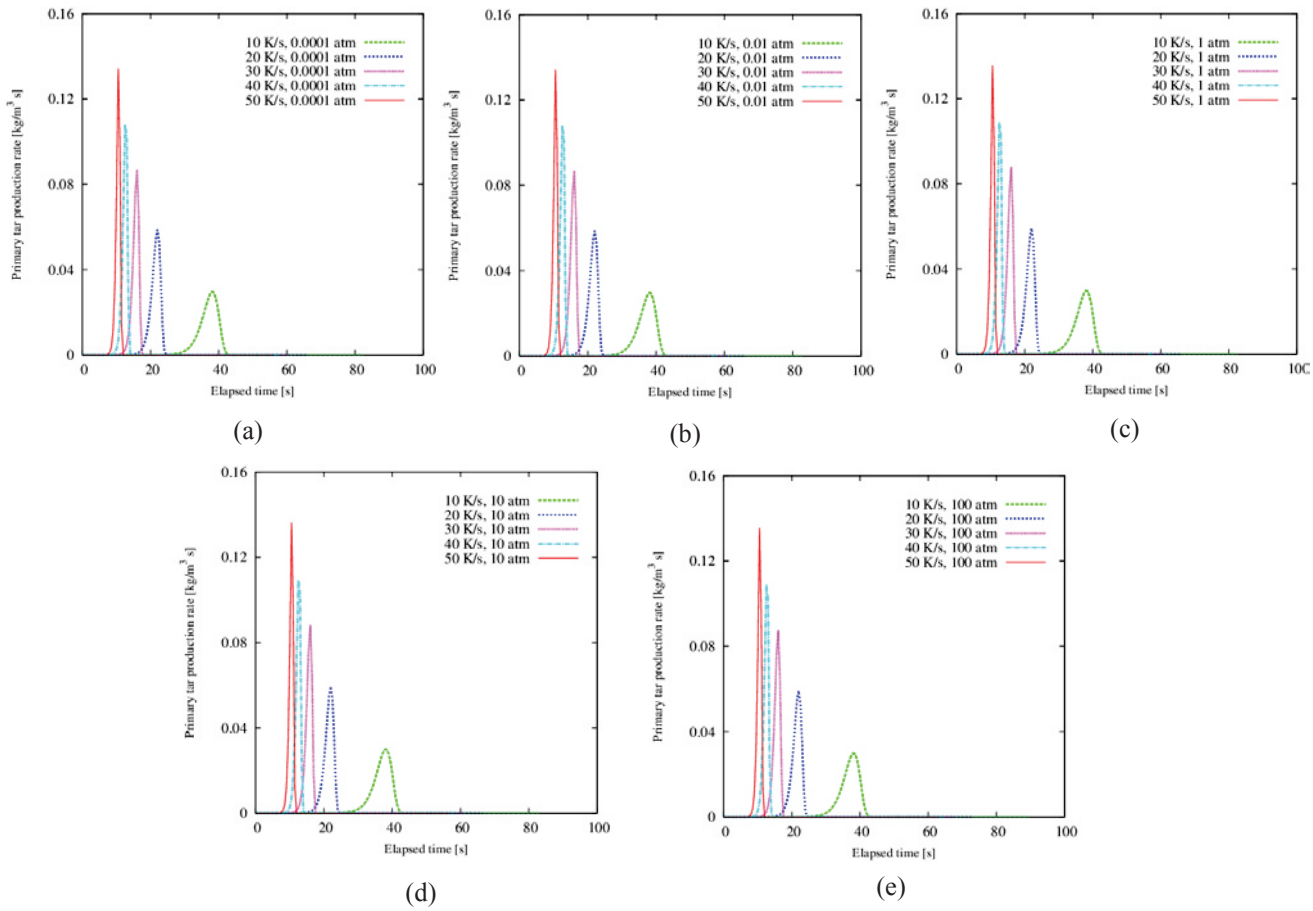

Figure 3: Primary tar production rate at different reactor pressures and heating rates

4.3 Secondary reactions products generation

Figure 4 [a-e] shows the rate of generation of secondary reactions products. From the figure, the rate of generation of secondary reactions products increased with increase in both heating rate and pyrolysis pressure. A closer look at this figure revealed that in the vacuum region (0.0001 and 0.01 atm), the highest peak was not at the highest heating rate. This may be due to the nature of intra-particle volatile transport and spatial temperature distribution in the pyrolyzing solid in this region as explained in our previous work [17]. As pressure increased from vacuum to atmospheric, the rate of generation of these products was doubled and much more than that at vacuum conditions for all heating rates. This is a little different from the results obtained in thermally thin regime, where the rates of generation of secondary reactions products at atmospheric condition were over ten times higher than those at vacuum conditions [17]. The difference resulted from the fact that in the thermally thin pyrolysis regime, the particle temperature is uniform and disintegration reaction takes place simultaneously throughout the particle [24], thereby enhancing secondary reactions due to high temperature and accelerated primary conversion of the particle. However, in thermally thick regime, there is significant spatial temperature distribution, resulting in an unreacted core surrounded by a layer of char separated by a thin reaction front, thereby slowing down the rate of sample conversion and of secondary reactions products evolution. As shown in the figure, further increase in pyrolysis pressure from atmospheric to pressurized conditions (10 and 100 atm) does not have any significant influence on the rate of secondary reactions products generation [Figure 4 (d & e)].

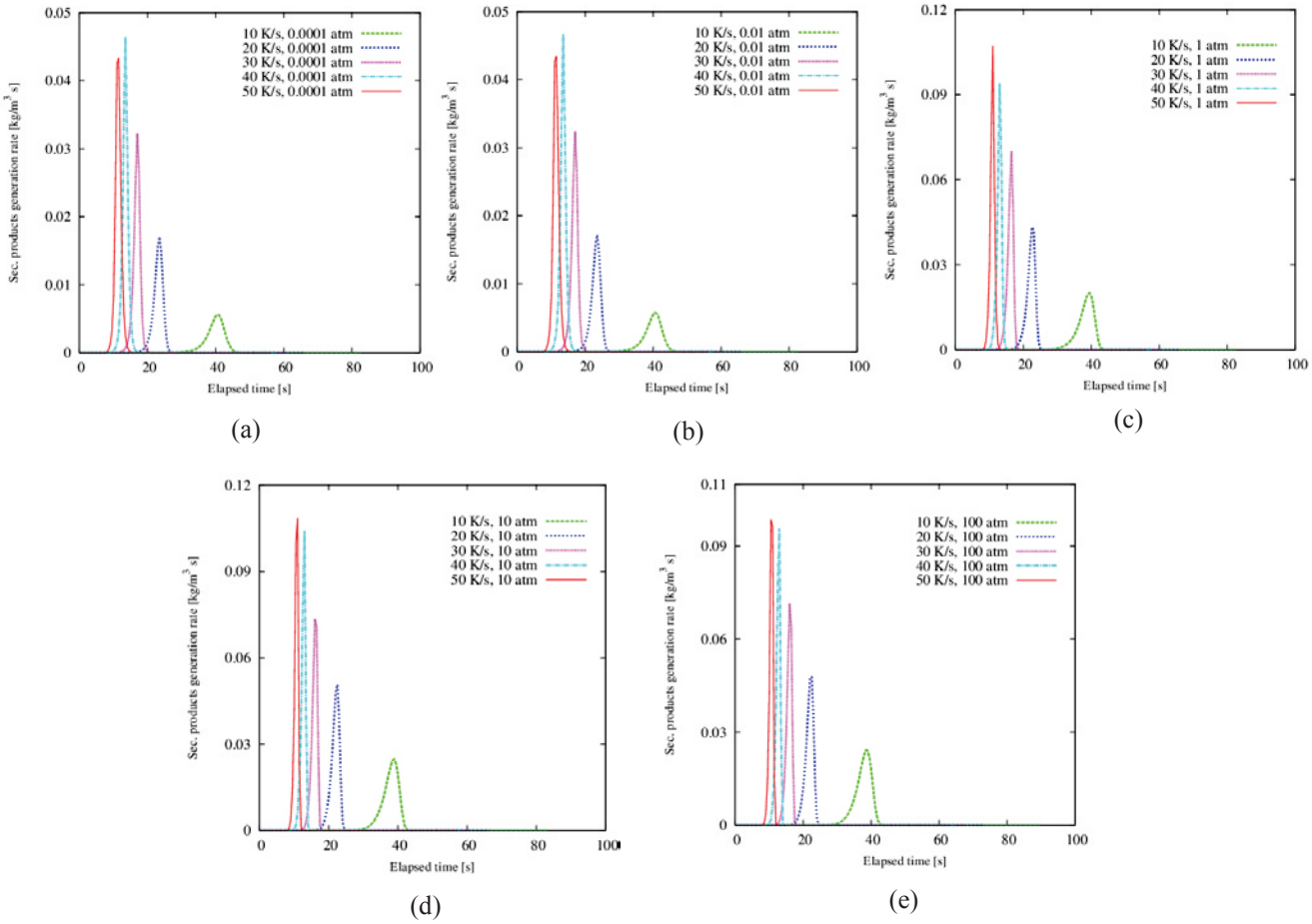

Figure 4: Rate of generation of secondary reactions products

4.4 Tar release rate

Figure 5 [a-e] shows the rate of primary tar release at different heating rates and pyrolysis pressure conditions. In all pyrolysis pressure regions considered, primary tar release rate increased with heating rate. As pressure increased from vacuum to atmospheric and from atmospheric to pressurized condition, however, primary tar release rate decreased at all heating rates. Furthermore, for all reactor pressures and heating rates considered, primary tar release, after reaching its peak did not only decline but also became negative. This negativity implies the consumption of tar molecules as they migrated through the heated char layer while attempting to escape to the surface of the pyrolyzing solid. Also, it could be seen from the figure that the negative peaks increased from vacuum to atmospheric condition [Figure 5(a-c)] and decreased from atmospheric to pressurized condition [Figure 5(c & d)] especially at higher heating rate (40 and 50 K/s), the highest peaks being at atmospheric condition. This implies that the quantity of tar molecules consumed increased as reactor pressure increased from vacuum to atmospheric condition and decreased as reactor pressure increased from atmospheric to pressurized condition. This scenario, most likely must have been due to pressure influence on tar intra-particle transport mechanism and secondary reaction kinetics. This is different from our findings in thermally thin regime where primary tar release rate declined consistently with pressure increase from vacuum to atmospheric condition and from atmospheric to pressurized condition without any negative peaks. This suggests that in thermally thick regime, tar molecules participate much more in intra-particle reactions. Further increase in reactor pressure in the pressurized region (10 to 100 atm) caused some more declination in the value of the negative peak at all heating rates [Figure 5(d & e)]. This suggests a reduction in the quantity of tar molecules consumed as they move through the heated char layer towards the surface of the pyrolyzing solid especially at higher heating rates (40 and 50 K/s). The extent of primary tar intra-particle secondary reactions is dependent on the synergetic effects of

reaction kinetics, spatial and temporal temperature distributions, and residence time. Even though increase in pressure will elongate tar residence time within the pyrolyzing solid, to the best of our knowledge, its effects on primary tar secondary reaction kinetics and intra-particle temperature distribution has not been clarified. In order to explain this result, an attempt was made to investigate the effect of pyrolysis pressure on temperature evolution at the centre of the pyrolyzing solid for all heating rates considered. Figure 6[a-e] shows the simulated temperature profiles at the centre of the particle. As seen from the figure, at the initial stage of pyrolysis, the centre temperature profile is the same at different pyrolysis pressures for all heating rates until at a point where pressure increase resulted in decrease in centre temperature gradient, the highest reactor pressure having the minimum temperature gradient. This decrease in temperature gradient with increase in pressure would have been responsible for decrease in the quantity of tar molecules consumed as pressure increased from atmospheric to pressurized condition and from 10 to 100 atm in the pressurized region. Further clarification of this scenario will be addressed in our subsequent studies.

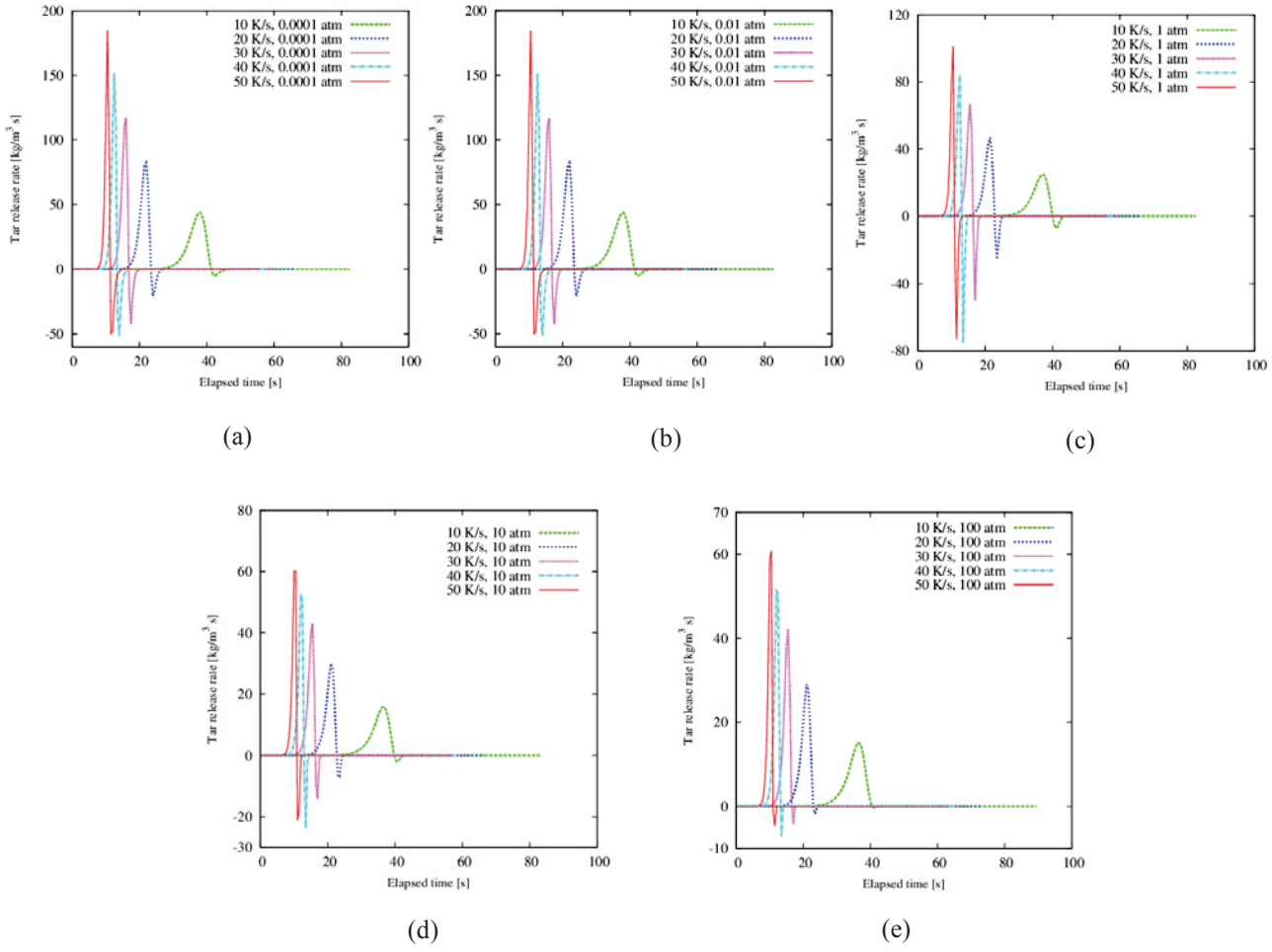

Figure 5: Tar release rate at different reactor pressures and heating rates

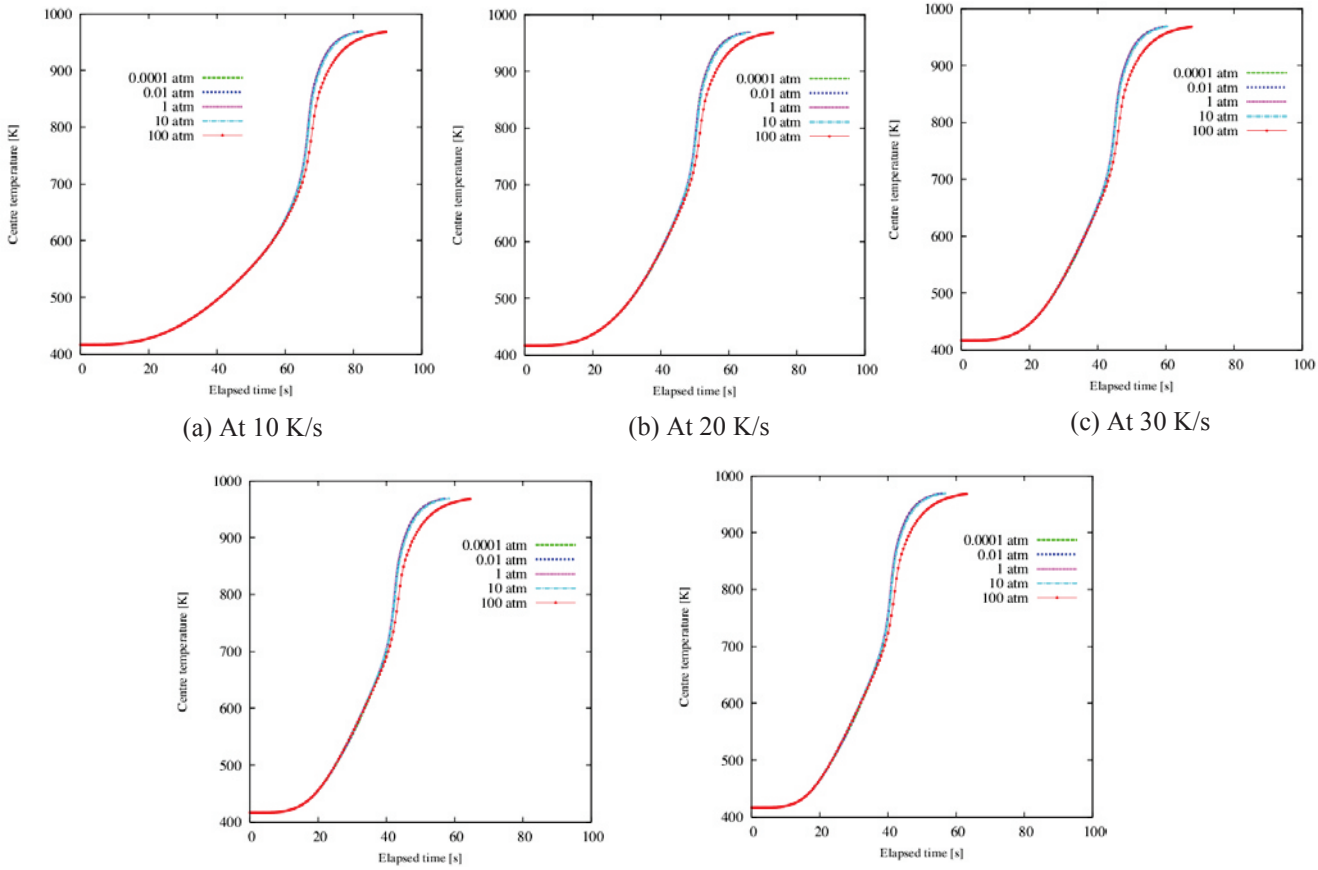

(a) At 10 K/s (b) At 20 K/s (c) At 30 K/s

(d) At 40 K/s (e) At 50 K/s

Figure 6: Centre temperature profiles at different reactor pressures and heating rates

4.5 Gas release rate

Figure 7 [a – e] shows the rate of gas release from the pyrolyzing solid at various pyrolysis pressure regions and at different heating rates. From the figure, it can be seen that gas release rate at vacuum, atmospheric and pressurized pyrolysis conditions increased with heating rate. In the vacuum region, increase in pressure (from 0.0001 to 0.01 atm) has no significant effect on gas release rates for all heating rates [Figure 7 (a & b)]. Increase in reactor pressure from vacuum to atmospheric condition [Figure 7 (b &c)] caused some increase in gas release rate at all heating rates. This is because pressure increase elongated volatiles residence time in the pyrolyzing solid thereby enhancing secondary reactions that led to more gas production. Further increase in reactor pressure from atmospheric to pressurized condition also caused more increase in gas release rate [Figure 7 (c & d)]. However, in the pressurized pyrolysis region, pressure increase (from 10 to 100 atm) has no noticeable effect on gas release rate [Figure 7(d & e)]. This result is similar to our findings in the thermally thin regime and detailed explanation has been given [17].

4.6 Intra-particle secondary reactions

In order to investigate the combined effect of pressure and heating rate on volatiles (mainly primary tar) intra-particle secondary reactions, the ratio of secondary reactions products release rate to primary tar production rate (R_s/R_p) was calculated. R_s and R_p have been defined earlier [21]. Figure 8 shows the variation of R_s/R_p at vacuum, atmospheric and pressurized pyrolysis conditions and at different heating rates. From the figure, it can

be seen that the minimum values of R_s/R_p were obtained at vacuum pyrolysis conditions (0.0001 and 0.01 atm). Within this region, increase in pressure did not have any clear influence on the ratio. This suggests that the reaction kinetics, volatile transport mechanism and intra-particle temperature distribution, all of which affect intra-particle secondary reactions, did not change despite the pressure increase in this region. On the contrary, as shown in the figure, the ratio R_s/R_p increased drastically with heating rate. This is different from our findings in the thermally thin regime [17], where increase in heating rate has no significant effect on R_s/R_p. As pyrolysis pressure increased from vacuum to atmospheric condition, R_s/R_p increased significantly, the increase also being sensitive to change in heating rate. Therefore, at atmospheric condition, the extent of intra-particle secondary reactions is much more than at vacuum conditions. This result is similar to our finding in thermally thin regime except that increase in heating rate has no significant effect on R_s/R_p. Increase in pyrolysis pressure from atmospheric (1 atm) to pressurized condition (10 atm) caused further increase in R_s/R_p until 40 K/s when the ratio is equal to that obtained at atmospheric condition. Above 40 K/s, R_s/R_p values at pressurized conditions began to fall below those obtained at atmospheric condition. Increase in reactor pressure (from 10 atm to 100 atm) in the pressurized region resulted in lower values of R_s/R_p than those obtained at 10 atm for all heating rates. Furthermore, as shown in Figure 8, the value of R_s/R_p obtained at 100 atm was equal to that obtained at atmospheric condition for heating rate of 30 K/s. Above 30 K/s, R_s/R_p values at 100 atm were lower than those obtained at 1 atm. This implies that the release rates of secondary reactions products at atmospheric condition were more than those at 100 atm above 30 K/s. This shows that the relationship between reactor pressure, heating rate and intra-particle secondary reactions in thermally thick regime is not linear. Therefore, to optimize biomass pyrolysis in thermally thick regime, depending on the preferred yield, a careful selection of reactor pressure and heating rate should be made. Our future works will address this.

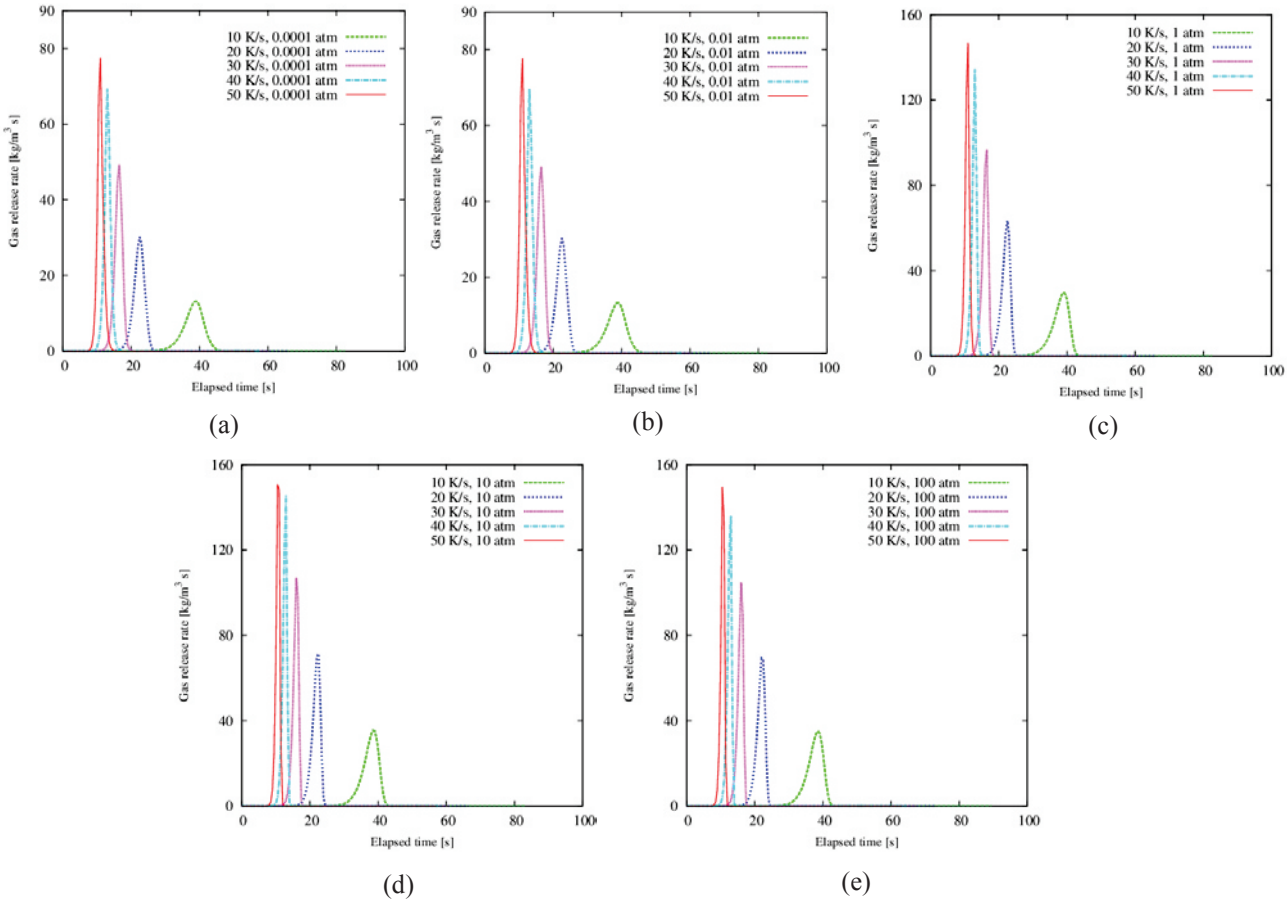

Figure 7: Gas release rate at different reactor pressures and heating rates

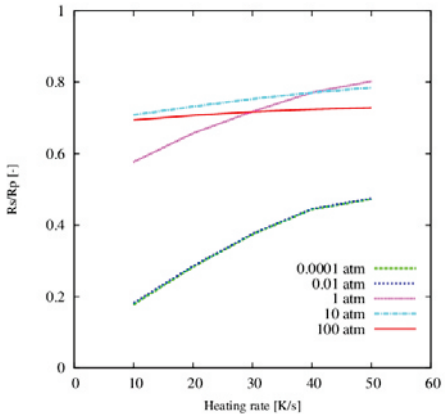

Figure 8: The ratio of the rate of primary tar secondary reactions products generation to the rate of primary tar production at different reactor pressures and heating rates

4.7 Final product yields

4.7.1 Total primary tar yield

Figure 9 shows tar yields at different reactor pressures and heating rates. From the figure, it is clear that maximum tar yields were collected at vacuum conditions for all heating rates and that tar yield decreased with increase in heating rate. Furthermore, as shown in the figure, pressure increase (from 0.0001 to 0.01 atm) within the vacuum region has no significant effect on total tar yields. As earlier explained, this result suggests that despite the pressure increase, the kinetics of secondary reactions, intra-particle temperature distribution and volatiles transport mechanism do not change significantly in the vacuum region. As reactor pressure increased from vacuum to atmospheric, total tar yields decreased significantly at all heating rates considered. It is expected that this decrease in tar yield will be accompanied with corresponding gas yield. Further increase in pressure from atmospheric to pressurized condition caused some further reduction in tar yield until 40 K/s when tar yield at 10 atm is equal to that at atmospheric condition (1 atm). Above 40 K/s, tar yield at 10 atm became higher than that at 1 atm. Pressure increase in the pressurized region (from 10 to 100 atm) does not cause any further decrease in total tar yields. In fact, total tar yields became higher at 100 atm than at 10 atm for all heating rates. It would also be observed that above 30 K/s, tar yields at 100 atm are higher than at atmospheric condition.

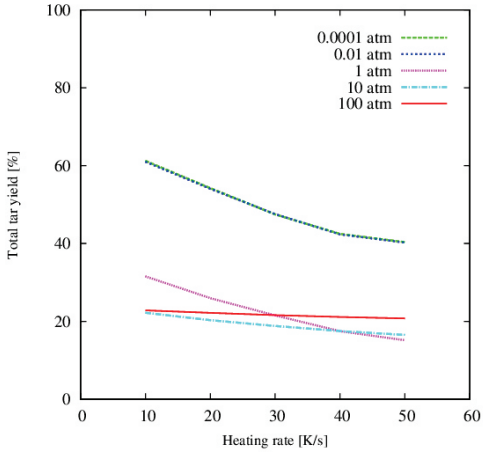

Figure 9: Effects of pressure and heating rate on total primary tar yield

These results are different from our findings when thermally thin pyrolysis regime was studied [17]. Plausible reasons for all these results have been explained in Section 4.6. Comparison of Figures 8 and 9 clearly reveals that the ratio R_s/R_p and total tar yield are inversely proportional.

4.7.2 Total gas yield

Figure 10 shows the total gas yields at different reactor pressures and heating rates. From the figure, as would be expected, lowest gas yields were collected in the vacuum region. Pressure increase in this region (from 0.0001 to 0.01) has no significant effect on gas yield. Pressure increase from vacuum (0.01 atm) to atmospheric (1 atm) caused a significant increase in gas yield at all heating rates. As the reactor pressure increased from atmospheric to pressurized condition (10 atm), total gas yield increased until 40 K/s when the total gas yield at 10 atm was the same as at atmospheric condition. Beyond 40 K/s, total gas yield at 10 atm was lower than at atmospheric condition. In the pressurized region, increase in reactor pressure (from 10 atm to 100 atm) caused total gas yields to fall below those at 10 atm at all heating rates. Moreover, beyond 30 K/s, total gas yields at 100 atm were lower than those at atmospheric condition. These results are in consonance with the trend reported in Section 4.6. Comparison of Figures 8 and 10 shows that R_s/R_p and total gas yield are directly proportional.

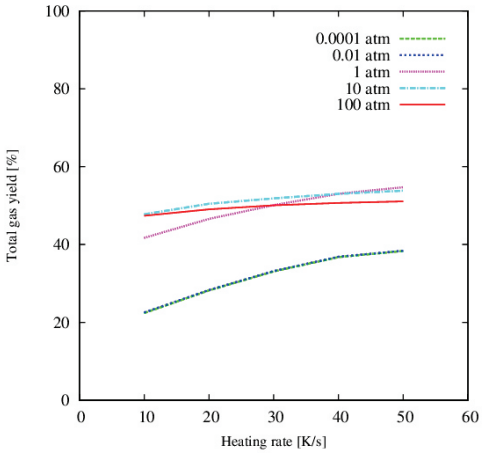

Figure 10: Effects of pressure and heating rate on total gas yield

4.7.3 Total char yield

Figure 11 shows the total char yields at various reactor pressures and heating rates. From the figure, total char yield in all pressure conditions were not significantly different. From weight loss profiles (Figure 2), this kind of result should be expected. The plausible reason may be due to the fact that extra-particle secondary reactions were not considered in this study.

4.7.4 Total secondary tar yield

Figure 12 shows the yield of total secondary tar at different pyrolysis pressures and heating rates. The lowest yields were obtained at vacuum condition (0.0001 atm). Pressure increase within vacuum region (from 0.0001 to 0.01 atm) has no effect on total secondary tar yield. As reactor pressure increased from vacuum to atmospheric condition, total secondary tar yield increased. Further increase in pressure from atmospheric to pressurized condition did not bring about any significant increase in secondary tar yield. In fact, as in gas yield, above 40 K/s, yields at 10 atm gradually declined below the yields at atmospheric pressure.

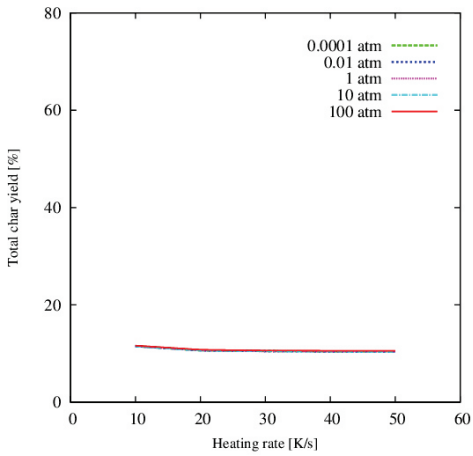

Figure 11: Effects of pressure and heating rate on total char yield

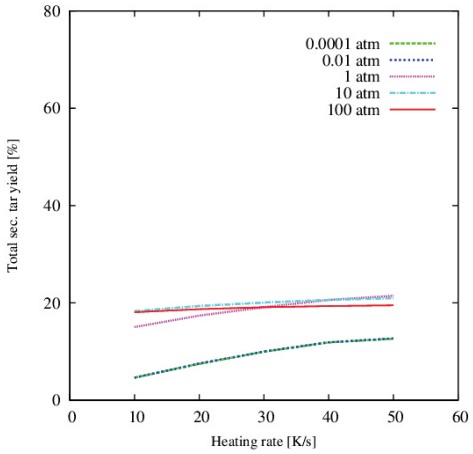

Figure 12: Effects of pressure and heating rate on secondary tar yield

5. Conclusions

The synergetic impact of pressure and heating rate in thermally thick pyrolysis regime has been numerically investigated at vacuum, atmospheric and pressurized conditions. Results showed that change in reactor pressure does not significantly influence biomass primary decomposition reactions. In the vacuum region, findings also revealed that increase in pressure did not significantly affect the release rates and yields of pyrolysis products. However, change in heating rate affected both evolution and total yields of tar, gas and char. Pressure increase from vacuum to atmospheric and from atmospheric to pressurized condition resulted in reduction in primary tar release rate and yield, increase in gas release rate and yield, and increase in secondary tar release rate and yield. Primary tar intra-particle secondary reactions were more sensitive to change in heating rate at vacuum conditions (0.0001 and 0.01 atm) than at atmospheric (1 atm) and pressurized (10 and 100 atm) conditions. Nevertheless, the degrees of volatiles intra-particle secondary reactions at atmospheric and pressurized conditions were much higher than at vacuum conditions (R_s/R_p values at atmospheric and pressurized conditions were almost three times higher than at vacuum conditions) for all heating rates. Depending on heating rate, the yield of primary tar at atmospheric pressure may be lower than that at pressurized conditions while the yield of gas and secondary tar may be higher. Char yields were not significantly different for all the pressure regions considered. Increase in heating rate, however, caused some slight reduction in char yield in all the pressure regions.

Nomenclature

A: pre-exponential factor (1/s)

B: permeability	(m^2)
Cp: specific heat capacity	(J/ kg K)
E: activation energy	(J/mol)
e: emissivity	(-)
h_c: convective heat transfer coefficient	(W/ m^2 K)
k: reaction rate constant	(1/s)
k_c: char thermal conductivity	(W/m K)
k_w: wood thermal conductivity	(W/m K)
M: molecular weight	(kg/mol)
P: Pressure	(Pa)
Q: heat generation	(W/m^3)
Q_c: convective heat flux	(W/m^2)
Q_r: radiation heat flux	(W/m^2)
R: universal gas constant	(J/mol K)
R: total radial length	(m)
r: radial direction	
z: axial direction	
S: source term	
T: temperature	(K)
t : time	(s)
U: axial velocity component	(m/s)
V: radial velocity component	(m/s)
ε: porosity	(-)
ε_0: initial porosity	(-)
Δh: heat of reaction	(kJ/kg)
μ: viscosity	(kg/m s)
ρ: density	(kg/m^3)
ρ_{w0}: initial density of wood	(kg/m^3)
σ: Stefan-Boltzmann constant	($W/m^2 K^4$)
η: degree of pyrolysis	

Subscripts
Ar: Argon
c: char, primary char formation reaction
c_2: secondary char formation reaction
g: gas, primary gas formation reaction
g_2: secondary gas formation reaction
is: intermediate solid, intermediate solid formation reaction
s: solid
t: tar, tar formation reaction
v: total volatile
w: wood

References

[1] Boroson, M.L., Howard, J.B., Longwell, J.P. & Peters, W.A. (1989). Product Yields and Kinetics from the Vapour Cracking of Wood Pyrolysis Tars. *AIChE***,** 35(1), 120-128.
[2] Miller, R.S. & Bellan, J. (1997) Tar Yield and Collection from the Pyrolysis of Large Biomass particles. *Combustion Science and Technology,* 127, 97-118.
[3] Cozzani, V., Nicolella, C., Rovatti, M. & Tognotti, L. (1996) Modeling and Experimental Verification of Physical and chemical Processes during Pyrolysis of a Refuse-Derived Fuel. *Industrial Engineering Chemistry Research,* 35(1): 90-98.
[4] Shafizadeh, F. and Bradbury, A.G.W. (1979) Thermal Degradation of Cellulose in Air and Nitrogen at Low Temperatures. *Journal of Applied Polymer Science*, 23, 1431-1442.
[5] Koufopanous, C.A. & Papayannakos, N. (1991) Modelling of the Pyrolysis of Biomass Particles. Studies on Kinetics, Thermal and Heat Transfer Effects. *The Canadian Journal of Chemical Engineering*, 69, 907-915.
[6] Li, Z., Liu, C., Chen, Z., Qjan, J., Zhao, W. & Zhu, Q. (2009)Analysis of Coal and Biomass Pyrolysis Using Distributed Activation Energy Model. *Bioresource Technology*, 100, 948-952.
[7] Miller, R.S. & Bellan, J. (1996) Analysis of Reaction Products and Conversion Time in the Pyrolysis of

Cellulose and Wood particles. *Combustion Science and Technology*, 119, 331-373.
[8] Di Blasi, C. (1996) Heat, Momentum and Mass Transport through a Shrinking Biomass particle Exposed to Thermal Radiation. *Chemical Engineering Science*, 51(7), 1121-1132.
[9] Haseli, Y., van Oijen, J.A. & de Goey L.P.H. (2011) Modeling Biomass Particle Pyrolysis with Temperature- Dependent Heat of Reactions. *Journal of Analytical and applied Pyrolysis*, 90, 140-154.
[10] Dufour, A., Ouartassi, B., Bounaceur, R. & Zoulalian, A. (2011) Modelling Intra-particle Phenomena of Biomass Pyrolysis. *Chemical Engineering Research and Design*, doi:10.1016/j.cherd.2011.01.005.
[11] Di Blasi, C. (1997) Influences of Physical Properties on Biomass Devolatilization Characteristics. *Fuel*, 76(10), 957-964.
[12] Okekunle, P.O. (2013) Numerical Investigation of the Effects of Thermo-physical Properties on Tar Intra-particle Secondary Reactions during Biomass Pyrolysis. *Mathematical Theory and Modeling*, 3(14), 83-97.
[13] Larfeldt, J., Leckner, B. & Melaaen, M.C. (2000) Modeling and Measurements of the Pyrolysis of Large Wood Particles. *Fuel*, 79, 1637-1643.
[14] Di Blasi, C., Signorelli, G., Di Russo, C. & Rea, G. (1999) Product Distribution from Pyrolysis of Wood and Agricultural Residues. *Industrial Engineering chemistry Research,* 38, 2216-2224.
[15] Lu, H., Ip, E., Scott, J., Foster, P., Vickers, M. & Baxter, L.L. (2010). Effects of Particle Shape and Size on Devolatilization of Biomass Particle. *Fuel,* 89, 1156-1168.
[16] Di Blasi, C. (2008) Modeling Chemical and Physical Processes of Wood and Biomass Pyrolysis. *Progress in Energy and Combustion Science*, 34, 47-90
[17] Okekunle, P.O., Osowade, E.A. & Oyekale, J.O. (2015) Numerical Investigation of the Combined Impact of Reactor Pressure and Heating Rate on Evolution and Yields of Biomass Pyrolysis Products in Thermally Thin Regime. *Journal of Energy Technologies and Policies*, 5(3), 93-106.
[18] Ståhl, M., Granström, K., Berghel, J. & Renström, R. (2004) Industrial Processes for Biomass Drying and their Effects on the Quality Properties of Wood Pellets. *Biomass and Bioenergy,* 27(6), 621-628.
[19] Becidan, M., Skreiberg, ø. & Hustad, J.E. (2007). Experimental Study on Pyrolysis of Thermally Thick Biomass Residues Samples: Intra-sample Temperature Distribution and Effect of Sample Weight (Scaling Effect). *Fuel*, 86, 2754-2760.
[20] Okekunle, P.O., Watanabe, H., Pattanotai, T. & Okazaki, K. (2012). Effect of Biomass Size and Aspect Ratio on Intra-particle Tar Decomposition during Wood Cylinder Pyrolysis. *Journal of Thermal Science and Technology* 7(1), 1-15.
[21] Okekunle, P.O., Pattanotai, T., Watanabe, H. & Okazaki, K. (2011). Numerical and Experimental Investigation of Intra-particle Heat Transfer and Tar Decomposition during Pyrolysis of Wood Biomass. *Journal of Thermal Science and Technology* 6(3), 360-375.
[22] Okekunle, P.O. & Osowade E.A. (2014). Numerical Investigation of the Effects of Reactor Pressure on Biomass Pyrolysis in Thermally Thin Regime. *International Journal of Chemical and Process Engineering Research,* 27, 12-22.
[23] Boroson, M.L., Howard, J.B., Longwell, J.P. & Peters, W.A. (1989). Heterogeneous Cracking of Wood pyrolysis Tars Over Fresh Wood Char Surfaces. *Energy & Fuels,* 3, 735-740.
[24] Hagge, M.J. and Bryden, K.M. (2002). Modeling the Impact of Shrinkage on the Pyrolysis of Dry Biomass. *Chemical Engineering Science,* 57, 2811-2823.